Kinetics and Mechanism of Alkyl Transfer from Organocobalt(III) to Nickel(I): Implications for the Synthesis of Acetyl Coenzyme A by CO Dehydrogenase

M. S. Ram,[†] Charles G. Riordan,*[,†] Glenn P. A. Yap,[‡] Louise Liable-Sands,[‡] Arnold L. Rheingold,[‡] Adam Marchaj,[§] and Jack R. Norton[§]

Contribution from the Departments of Chemistry, Kansas State University, Manhattan, Kansas 66506, University of Delaware, Newark, Delaware 19716, and Colorado State University, Fort Collins, Colorado 80523

Received August 30, 1996[⊗]

Abstract: Reaction of $CH_3Co(dmgBF_2)_2L$ ($dmgBF_2$ = (difluoroboryl)dimethylglyoximato); L = py, PEt_3) with 2 equiv of [Ni(tmc)]OTf (tmc = 1,4,8,11-tetramethyl-1,4,8,11-tetraazacyclotetradecane; OTf^- = $CF_3SO_3^-$) gave $Co(dmgBF_2)_2py^-$, $[Ni(tmc)]OTf_2$, and $[Ni(tmc)CH_3]OTf$ in 80% yield. The overall transformation provides the first model for the transfer of a CH_3 group from methylcobalamin to the Ni-containing enzyme carbon monoxide dehydrogenase during acetyl coenzyme A synthesis. *RRSS*−$[Ni(tmc)CH_3](BAr'_4)$ ($BAr'_4{}^-$ = $B(3,5\text{-}(CF_3)_2C_6H_3)_4^-$) has been characterized by X-ray diffraction. The products and $1CH_3Co(dmgBF_2)_2L$:2[Ni(tmc)]OTf stoichiometry of the reaction are consistent with a three-step mechanism initiated by electron transfer from [Ni(tmc)]OTf to CH_3-$Co(dmgBF_2)_2L$. The second step is rapid CH_3-Co^- bond homolysis yielding $Co(dmgBF_2)_2L^-$ and $CH_3\bullet$; then the CH_3 radical is captured by the second equivalent of [Ni(tmc)]OTf, yielding $[Ni(tmc)CH_3]OTf$. Radical clock experiments have corroborated the production of free radicals. Reaction of (5-hexenyl)$Co(dmgBF_2)_2L$ with [Ni-(tmc)]OTf, followed by hydrolysis of the organonickel products, gave methylcyclopentane, consistent with the formation and cyclization of the 1-hexenyl radical. The second-order rate constants measured by stopped-flow experiments parallel the relative radical stabilities: R = CH_3 (2.43×10^3 M^{-1} s^{-1}) < C_2H_5 (7.88×10^3 M^{-1} s^{-1}) < $CH(CH_3)_2$ (19.2×10^3 M^{-1} s^{-1}), L = py (2.43×10^3 M^{-1} s^{-1}) < PEt_3 (5.01×10^3 M^{-1} s^{-1}). During the course of these studies the following molecules were also characterized by X-ray diffraction, $CH_3Co(dmgBF_2)_2L$, L = PEt_3, py, H_2O.

Introduction

The nickel-containing enzyme carbon monoxide dehydrogenase (CODH), found in certain methanogenic, acetogenic, and sulfate-reducing bacteria, enables these species to grow autotrophically by the catalysis of two distinct reactions, the oxidation of CO to CO_2 and the synthesis of acetyl-coenzyme A (acetyl-CoA) via the Wood−Ljungdahl pathway.[1] The latter process, termed acetyl-CoA synthetase (ACS), requires the multistep coupling of a CH_3 group from a corrinoid protein (C/Fe-SP) to CO and the thiolate, CoA.[2] CODH has been subjected to a complete array of spectroscopic studies which have resulted in the development of working models for the active sites of CO oxidation (cluster C) and acetyl-CoA synthesis (cluster A).[3] Both contain unusual heterometallic clusters in which a single nickel ion is covalently linked by a bridging ligand, X (S^{2-} or RS^- from a cysteine residue), to a $[Fe_4S_4]^{2+/+}$ cluster. However, the nickel primary coordination sphere ligand composition and geometry appear different for the two sites. The nickel in cluster A resides in a distorted planar S_4 or S_2N_2 donor environment. Spectroelectrochemical and EPR studies suggest that CO and CH_3 bind to the same state of the enzyme, which is one electron reduced from the resting state.[4] Vibrational spectroscopy has provided a detailed picture of the CO and CH_3 binding loci within cluster A.[5] CO is terminally bound to an iron and the CH_3 is bound to nickel as kinetically competent intermediates. Consequently, Ragsdale, Spiro, and co-workers have proposed[5a] a bimetallic catalytic mechanism reminiscent of the Monsanto acetic acid cycle. Notable features of the mechanism include nonenzymatic transfer of a methyl substituent from methylcobalamin to nickel; bimetallic migratory insertion producing an iron (or nickel) acetyl; and nucleophilic attack on the acetyl by CoA or, alternatively, coordination of CoA to cluster A, yielding a metal thiolate, followed by formal reductive elimination of acetyl-CoA.

Model studies using mononuclear nickel species have reproduced many of the proposed steps in the catalytic cycle.[6] Holm has employed Sacconi's NS_3 tripodal ligand (NS_3 = $N(CH_2$-

* To whom correspondence should be addressed. E-mail: Riordan@ksu.edu.
[†] Kansas State University.
[‡] University of Delaware
[§] Colorado State University.
[⊗] Abstract published in *Advance ACS Abstracts,* January 15, 1997.

(1) (a) Ragsdale, S. W. *Crit. Rev. Biochem. Mol. Biol.* **1991**, *26*, 261−300. (b) *The Bioinorganic Chemistry of Nickel*; Lancaster, J. R., Ed.; VCH Publishers: New York, 1988; Chapters 13 and 14.

(2) (a) Ljungdahl, L. G. *Annu. Rev. Microbiol.* **1986**, *40*, 415. (b) Fuchs, G. *FEMS Microbiol. Rev.* **1986**, *39*, 181−213. (c) Wood, H. G.; Ragsdale, S. W.; Pezacka, E. *Trends Biochem. Sci.* **1986**, *11*, 14.

(3) (a) Cramer, S. P.; Eidsness, M. K.; Pan, W.; Morton, T. A.; Ragsdale, S. W.; DerVartanian, D. V.; Ljungdahl, L. G.; Scott, R. A. *Inorg. Chem.* **1987**, *26*, 2477−2479. (b) Bastian, N. R.; Diekert, G.; Niederhoffer, E. G.; Teo, B.; Walsh, C. P.; Orme-Johnson, W. H. *J. Am. Chem. Soc.* **1988**, *110*, 5581−5582. (c) Lindahl, P. A.; Ragsdale, S. W.; Münck, E. *J. Biol. Chem.* **1990**, *265*, 3880−3888. (d) Fan, C.; Gorst, C. M.; Ragsdale, S. W.; Hoffman, B. M. *Biochemistry* **1991**, *30*, 431−435. (e) Xia, J.; Dong, J.; Wang, S.; Scott, R. A.; Lindahl, P. A. *J. Am. Chem. Soc.* **1995**, *117*, 7065−7070.

(4) Lu, W.; Harder, S. R.; Ragsdale, S. W. *J. Biol. Chem.* **1990**, *265*, 3124−3133.

(5) (a) Qiu, D.; Kumar, M.; Ragsdale, S. W.; Spiro, T. G. *Science* **1994**, *264*, 817−819. (b) Kumar, M.; Qiu, D.; Spiro, T. G.; Ragsdale, S. W. *Science* **1995**, *270*, 628−630.

(6) (a) Stavropoulos, P.; Carrié, M.; Muetterties, M. C.; Holm, R. H. *J. Am. Chem. Soc.* **1990**, *112*, 5385−5386. (b) Stavropoulos, P.; Carrié, M.; Muetterties, M. C.; Holm, R. H. *J. Am. Chem. Soc.* **1991**, *113*, 8485−8492. (c) Matsunaga, P.; Hillhouse, G. L. *Angew. Chem., Int. Ed. Engl.*

S0002-7863(96)03061-2 CCC: $14.00

$CH_2SR)_3$, R = Pr^i, Bu^t) to prepare *tbp* $Ni(NS_3)X^+$ derivatives including X = CH_3. The methyl complex reacts with CO to yield isolable $(NS_3)NiC(O)CH_3^+$, which subsequently reacts with thiols producing $CH_3C(O)R$, Ni(0), and HNS_3^+.[6a,b] The latter reaction is proposed to occur via nucleophilic attack of the thiolate on the acetyl ligand. Hillhouse has used planar (bpy)NiSCH$_2$CH$_2$CH$_2$ to produce thialactones under a CO atmosphere.[6c] Recently, Holm has demonstrated CO insertion into the CH_3−Ni bond of $(bpy)NiCH_3(SR)$ yielding the first stable acetyl(thiolato)nickel complex.[6d] Additional exposure to CO results in reductive elimination of $CH_3C(O)SR$. The latter two studies provide precedent for nickel-mediated intramolecular thioester formation.

While these studies provide a model for several of the stoichiometric transformations relevant to ACS activity, precedents for alkyl transfer from cobalt to nickel have not existed in the organometallic literature. The studies contained herein describe a successful strategy that provides the first example of methyl transfer from CH_3Co to Ni(I) yielding a stable CH_3-Ni species.[7] Stopped-flow and radical clock experiments have suggested a detailed mechanism. The results obtained on these model systems are critically evaluated in the context of the parameters of ACS catalysis. Additionally, we have elucidated the structures of the organocobalt complexes and *RRSS*-[Ni(tmc)CH_3](BAr'_4) by X-ray diffraction.

Experimental Section

Materials and Methods. All manipulations were carried out under N_2 or Ar using standard Schlenk and glovebox techniques. All solvents were purified as previously described.[8] NMR solvents were obtained from Cambridge Isotope Labs and were used without further purification. PEt_3 and 1-bromo-5-hexene were used as received from Aldrich. NMR spectra were recorded on a 400-MHz Varian Unity Plus equipped with a Sun workstation. Samples of [Ni(tmc)CH_3](X) required 10 mM concentrations and 2K transients to obtain adequate signal-to-noise ratios. Twenty hertz line broadening was used for processing the paramagnetic ^{1}H NMR spectra. One hertz line broadening was used to process the ^{2}H, ^{13}C, and ^{19}F data. GC−MS experiments were performed on a Hewlett-Packard 5989A mass spectrometer interfaced with a HP 5890-II gas chromatograph. Cyclic voltammetric experiments were performed on a BAS 50W voltammetric analyzer employing cells housed inside a Vacuum Atmospheres glovebox.[8] Experiments at sweep rates exceeding 2 V/s were performed on a BAS 100 voltammetric analyzer using a 50-μm Pt wire working electrode.[9] Potentials were referenced to internal ferrocene/ferrocenium (Fc/Fc^+, $E_{1/2}$ = +801 mV vs NHE in THF). $(CH_3)_2Mg$ was prepared by stirring CH_3MgBr in Et_2O with 1 equiv of dioxane; the $MgBr_2$ was filtered off and $(CH_3)_2Mg$ was used as a stock solution. $NaBAr'_4$ and $NaB(C_6F_5)_4$ were prepared according to Brookhart[10] and characterized by ^{19}F NMR ($(CH_3)_2CO$, 27 °C): $NaBAr'_4$ δ 10.2 (s, CF_3); $NaB(C_6F_5)_4$ δ −94.6 (t, 8 F), −91.4 (t, 4 F), −62.4 (d, 8 F). *RRSS*- and *RSRS*-[Ni(tmc)]OTf_2 were synthesized as described by Barefield.[11] The PF_6^- salts were prepared from the OTf^- salts as previously described.[8] Ni(tmc)(OTf)•NaOTf was prepared as previously described[7] and was characterized by its electronic spectrum in THF (ϵ(352 nm) = 3700 M^{-1} cm^{-1}). $Co(dmgBF_2)_2(H_2O)_2$ was prepared in THF rather than Et_2O as described by Bakac and Espenson.[12]

***RRSS*- and *RSRS*-[Ni(tmc)CH_3](X) (X = OTf^-, $B(C_6H_5)_4^-$, $B(C_6F_5)_4^-$, $B(3,5\text{-}(CF_3)_2C_6H_3)_4^-$($BAr'_4^-$), and PF_6^-).** The synthesis of each isomer proceeded similarly. [Ni(tmc)]$(B(C_6F_5)_4)_2$ and [Ni(tmc)]-$(BAr'_4)_2$ were prepared by methathesis of [Ni(tmc)]OTf_2 with the corresponding Na salt in acetone. The final products were washed with hexanes containing 5% EtOH and then with hexanes containing 5% Et_2O. [Ni(tmc)]$(B(C_6F_5)_4)_2$ and [Ni(tmc)]$(BAr'_4)_2$ are soluble in THF. The appropriate [Ni(tmc)]$(X)_2$ (1.0 g, 1.6 mmol) was reacted with $(CH_3)_2Mg$ (50% excess) in 1:1 THF−Et_2O. The Mg salts were separated by filtration and the solvents were removed in vacuo. [Ni(tmc)CH_3](BAr'_4) was recrystallized from Et_2O−hexanes. [Ni(tmc)-CH_3](BAr'_4) and [Ni(tmc)CH_3]$(B(C_6F_5)_4)$ were soluble in THF, Et_2O, and $(CH_3)_2CO$. In general, the *RRSS* derivatives were less soluble than the *RSRS* species. Yields: 60%. UV−vis (THF), λ_{max}, nm (ϵ, M^{-1} cm^{-1}): 352 (1700), 705 (40). ^{1}H NMR ($(CD_3)_2SO$, 27 °C): *RRSS*-[Ni(tmc)CH_3][$B(C_6H_5)_4$] δ 123.10, 101.28, 75.07, 51.83, 32.57, 7.19 (m, $B(C_6H_5)_4$), 6.93 (m, $B(C_6H_5)_4$), 6.80 (m, $B(C_6H_5)_4$), −3.47, −7.47, −332 (Ni−CH_3); *RRSS*-[Ni(tmc)CH_3][OTf], ^{13}C δ 163.3, 139.4, 99.43, 74.96, 50.13, 34.83, 31.37, 17.10, −3.17, −5.40, −7.40, −11.6, −14.2, −332 (Ni−CH_3).

R$Co(dmgBF_2)_2$L (R = CH_3, CH_2CH_3, $CH(CH_3)_2$, $(CH_2)_4CH{=}CH_2$; L = py, PEt_3, H_2O). These complexes were originally prepared by Schrauzer[14] from $CH_3Co(dmgH)_2L$ and BF_3•Et_2O. We found it more efficient to prepare these complexes from $Co(dmgBF_2)_2(H_2O)_2$ in the presence of L by standard reduction/alkylation procedures as exemplified for $CH_3Co(dmgBF_2)_2$py: $Co(dmgBF_2)_2(H_2O)_2$ (1.0 g, 2.4 mmol) was suspended in 40 mL of CH_3OH in a Schlenk flask under Ar. NaOH (0.2 mL, 50%) was added followed by addition of py (0.2 mL, 2.5 mmol). The mixture was cooled to 10 °C and $NaBH_4$ (0.15 g, 4.0 mmol) was added. The mixture was stirred for 5 min during which time the color changed from brown to blue-green. $(CH_3)_2SO_4$ (0.8 mL, 8.4 mmol) was added and the solution turned yellow over 10 min. The remaining procedures were carried out under ambient conditions. An additional 1.0 mL of py was added and the solution stirred for 5 min. Fifty milliliters of H_2O was added, and the product was filtered and washed with 3 × 20 mL of H_2O. Alternately, $CH_3Co(dmgBF_2)_2PEt_3$ was prepared from $CH_3Co(dmgBF_2)_2H_2O$ by reaction with PEt_3 in CH_2Cl_2. The (5-hexenyl)Co derivatives were prepared from 1-bromo-5-hexene in CH_3CN. Products were recrystallized from CH_2Cl_2−Et_2O. Yields: greater than 80%. Electronic spectra agreed with those reported.[12] ^{1}H NMR (CD_3NO_2, 27 °C): $((CH_3)_2CH)Co(dmgBF_2)_2$py δ 7.85(d, py, 2 H), 7.73 (t, py, 1 H), 7.38 (t, py, 2 H), 2.54 (s, CH_3, 12 H), 2.19 (sept, CH, 1 H), 0.38 (d, $CH(CH_3)_2$, 6 H); $(CH_3CH_2)Co(dmgBF_2)_2$py δ 7.90 , 7.42 (py, 5 H), 2.45 (s, CH_3, 12 H), 2.18 (q, CH_2CH_3, 2 H), 0.26 (t, CH_2CH_3, 3 H). ^{1}H NMR ($(CD_3)_2CO$, 27 °C): (5-hexenyl)$Co(dmgBF_2)_2$py δ 8.04 (d, py, 2 H), 7.91 (t, py, 1 H), 7.41 (t, py, 2 H), 5.75 (m, CH, 1 H), 4.92 (m, $CHCH_2$, 2 H), 2.46 (s, CH_3, 12 H), 1.96 (q, CH_2, 2 H), 1.26 (q, CH_2, 2 H), 0.88 (m, CH_2, 2 H); (5-hexenyl)$Co(dmgBF_2)_2PEt_3$ δ 5.72 (m, CH, 1 H), 4.87 (m, $CHCH_2$, 2 H), 2.40 (d, $^5J_{P-H}$ = 4.27 Hz, CH_3, 12 H), 2.13 (m, CH_2, 2 H), 1.94 (q, CH_2, 2 H), 1.63 (m, $^2J_{P-H}$ = 8.3 Hz, PCH_2, 6 H), 1.24 (q, CH_2, 2 H), 0.94 (m, $^3J_{P-H}$ = 13.4 Hz, PCH_2CH_3, 9 H), 0.64 (q, CH_2, 2 H). In coordinating solvents such as CH_3CN or $(CH_3)_2SO$, $CH_3Co(dmgBF_2)_2$py exists as a 1:1 equilibrium mixture of $CH_3Co(dmgBF_2)_2$py and $CH_3Co(dmgBF_2)_2S$. ^{1}H NMR ($(CD_3)_2SO$, 27 °C): $CH_3Co(dmgBF_2)_2((CH_3)_2SO)$ δ 2.12 (s, CH_3, 12 H), 0.88 (s, CH_3Co, 3 H). $CH_3Co(dmgBF_2)_2PEt_3$ showed no evidence of ligand exchange in these solvents.

Conversion of $CH_3Co(dmgBF_2)_2$py to $CH_3Co(dmgBF_2)_2H_2O$. $CH_3Co(dmgBF_2)_2$py was washed three times with 20 mL of 6 M $HClO_4$ and subsequently washed with two times with 20 mL of H_2O. $CH_3Co(dmgBF_2)_2H_2O$ was precipitated from 1:1 ethyl acetate−$(CH_3)_2CO$ upon addition of 1:1 Et_2O−hexanes. The aquo complex is highly soluble in $(CH_3)_2CO$. This procedure is efficient in eliminating $Co(dmgBF_2)_2(H_2O)_2$, a common contaminant in the $RCo(dmgBF_2)_2$py complexes.

1994, 1748−1750. (d) Tucci, G. C.; Holm, R. H. *J. Am. Chem. Soc.* **1995**, *117*, 6489−6496. (e) Sellmann, D.; Schillinger, H.; Knoch, F.; Moll, M. *Inorg. Chim. Acta* **1992**, *198*, 351. (f) Sellmann, D.; Häussinger, D.; Knoch, F.; Moll, M. *J. Am. Chem. Soc.* **1996**, *118*, 5368−5374.

(7) Ram, M. S.; Riordan, C. G. *J. Am. Chem. Soc.* **1995**, *117*, 2365−2366.

(8) Ram, M. S.; Riordan, C. G.; Ostrander, R.; Rheingold, A. L. *Inorg. Chem.* **1995**, *34*, 5884−5892.

(9) Wightman, R. M.; Wipf, D. O. In *Electroanalytical Chemistry, A Series of Advances*; Bard, A. J., Ed.; Marcel Dekker: New York, 1987; Vol. 15, p 328.

(10) Brookhart, M.; Grant, B.; A. F. Volpe, J. *Organometallics* **1992**, *11*, 3920−3922.

(11) (a) Wagner, F.; Barefield, E. K. *Inorg. Chem.* **1973**, *12*, 2435−2439. (b) Wagner, F.; Barefield, E. K. *Inorg. Chem.* **1976**, *15*, 408−417.

(12) Bakac, A.; Espenson, J. H. *J. Am. Chem. Soc.* **1984**, *106*, 5197−5202.

(13) Lin, S.; Juan, B. *Helv. Chim. Acta* **1991**, *74*, 1725.

(14) Schrauzer, G. N. *Acc. Chem. Res.* **1968**, *1*, 97−103.

Table 1. Crystallographic Data

	[Ni(tmc)CH_3](BAr'_4)	$CH_3Co(dmgBF_2)_2(PEt_3)$	$CH_3Co(dmgBF_2)_2(py)\bullet 2CH_3NO_2$	$CH_3Co(dmgBF_2)_2(H_2O)$
formula	$C_{47}H_{47}BF_{24}N_4Ni$	$C_{15}H_{30}B_2CoF_4N_4O_4P$	$C_{16}H_{26}B_2CoF_4N_7O_8$	$C_9H_{17}B_2CoF_4N_4O_5$
formula weight	1193.4	517.9	601.0	417.82
color, habit	emerald green block	brown block	orange block	red block
crystal system	orthorhombic	tetragonal	orthorhombic	orthorhombic
space group	Pbca	$I4_1/a$	Pbca	Pbca
a, Å	19.036(2)	31.654(4)	19.648(2)	12.551(3)
b, Å	19.890(2)	31.654(4)	9.789(2)	12.952(3)
c, Å	27.737(2)	18.331(7)	35.969(5)	19.390(2)
V, Å^3	10502(1)	18336(3)	5158(1)	3152(1)
Z	8	32	8	8
T, K	296	247	298	248
λ, Å (Mo Kα)	Cu Kα (1.54178)	Mo Kα (0.71073)	Mo Kα (0.71073)	Mo Kα (0.71073)
ρ(calcd), g cm^{-3}	1.510	1.499	1.548	1.761
μ, cm^{-1}	16.53	8.78	7.49	11.63
$R(F)$, $R(wF^2)$[a]	0.0847, 0.2011[a]	0.0586, 0.1365[a]	0.0732, 0.1596[a]	0.0523, 0.1373[a]

[a] $R(F) = \sum\Delta/\Sigma(F_o)$, $\Delta = |F_o - F_c|$; $R(wF^2) = \sum[w(F_o^2 - F_c^2)^2]/\sum[(wF_o^2)^2]^{1/2}$.

Reconversion to $CH_3Co(dmgBF_2)_2py$. Pyridine (0.3 g) was added to aqueous $CH_3Co(dmgBF_2)_2H_2O$. After 15 min a yellow precipitate formed and was isolated by filtration and washed with 1:1 Et_2O−hexanes containing 1% py. Yield: 80%. The pyridine complex is moderately soluble in $(CH_3)_2CO$, CH_2Cl_2, $(CH_3)_2SO$, and CH_3CN. ^{1}H NMR ($(CD_3)_2CO$, 27 °C): δ 8.06 (d, py, 2 H), 7.92 (t, py, 1 H), 7.43 (t, py, 2 H), 2.44 (s, C*H*$_3$, 12 H), 1.25 (s, C*H*$_3$Co, 3 H).

Na[Co(dmgBF$_2$)$_2$(L)] (L = py, PEt$_3$). $Co(dmgBF_2)_2(H_2O)_2$ (500 mg, 1.2 mmol) was added to PEt_3 (1.25 mL, 1 M in THF) in 20 mL of THF. The mixture was vigorously stirred over Na/Hg (60 g 0.33%) for 20 min. The THF solution was filtered through Celite. The product was precipitated by addition of 20 mL of Et_2O and 100 mL of hexanes and subsequently washed with Et_2O (3 × 20 mL). Recrystallization from THF−Et_2O yielded 75% of Na[Co(dmgBF$_2$)$_2$(PEt$_3$)]. Na[Co(dmgBF$_2$)$_2$(py)] was prepared in an analogous manner. Na[Co(dmgBF$_2$)$_2$(PEt$_3$)]: ^{1}H NMR ($(CD_3)_2CO$, 27 °C) δ 1.89 (s, C*H*$_3$, 12 H), 1.34 (q, PC*H*$_2$, 6 H), 0.75 (t, PCH$_2$C*H*$_3$, 9 H); UV−vis (acetone), λ_{max}, nm (ϵ, M^{-1} cm^{-1}) 622 (9500). ^{1}H NMR ($(CD_3)_2SO$, 27 °C): δ 8.06 (d, py, 2 H), 7.92 (t, py, 1 H), 7.43 (t, py, 2 H), 1.76 (s, C*H*$_3$, 12 H); UV−vis (acetone), λ_{max}, nm (ϵ, M^{-1} cm^{-1}) 640 (9500).

Reactions of [Ni(tmc)CH$_3$]OTf. [Ni(tmc)CH_3]OTf was characterized by its reactions with H_2O (D_2O) and $HgCl_2$. Hydrolysis of [Ni(tmc)CD_3](OTf) (prepared from $(CD_3)_2Mg$) with H_2O in $(CH_3)_2SO$ yielded [Ni(tmc)OH](OTf)[15] and CD_3H. ^{1}H NMR ($(CD_3)_2SO$, 27 °C): δ 0.14 (sept, $^2J_{H-D} = 1.95$ Hz, CD_3H). [Ni(tmc)CH_3]OTf (60 mg, 0.13 mmol) reacted with $HgCl_2$ (40 mg, 0.14 mmol) in 2 mL of $(CH_3)_2SO$ to yield a red solution and white precipitate. ^{1}H NMR of red solution ($(CD_3)_2SO$, 27 °C): δ 0.75 (t, $^2J_{^{199}Hg-H} = 222$ Hz, C*H*$_3$HgCl).

Stopped-Flow Experiments. The stopped-flow system was configured and used as described elsewhere[16] with the following modifications. An On-Line Instrument Systems RSM 1000 rapid scanning monochromator was used to scan the UV−vis region at 1-ms intervals over an adjustable 300-nm wavelength range. The system was controlled and the spectral and kinetic data were analyzed with OLIS RSM software on a Dell 4100 DM microcomputer. The reagent solutions were prepared and handled under Ar at 25 ± 0.1 °C. [Ni(tmc)]OTf was always present in at least 10-fold excess. For each set of reagent concentrations, data from about six kinetic runs were collected and the observed rate constants averaged.

GC−MS Experiments. Methane was separated on a 10" Carbosphere column (130 °C) with N_2 as carrier gas using a TCD. In a representative experiment, $CH_3Co(dmgBF_2)_2L$ (1.0 mM) was reacted with [Ni(tmc)]OTf (2.0 mM) in $(CH_3)_2SO$ followed by hydrolysis in a 5-mL glass vial with a screw cap injection valve. CH_4 was produced in greater than 80% yield based on standard reactions (CH_3MgBr hydrolysis) at similar concentrations. Organic products from reactions of (5-hexenyl)Co(dmgBF$_2$)$_2$L with [Ni(tmc)]OTf in $(CH_3)_2SO$ for L = py (or $(CH_3)_2CO$ for L = PEt_3) followed by hydrolysis were monitored as follows. In $(CH_3)_2SO$, 1-hexene (retention time = 1.75 min) and methylcyclopentane (2.05 min) were resolved on a nonpolar RTX-1 column (30 m × 0.25 mm, 50 °C). In $(CH_3)_2CO$, it was necessary to ramp the oven temperature (30 °C, 2 min−50 °C/min−50 °C, 8 min−50 °C/min−300 °C) to minimize interference from the solvent. Under these conditions retention times were 4.10 min for 1-hexene and 5.10 min for methylcyclopentane. In both cases, GC peaks were analyzed by mass selection. While both 1-hexene and methylcyclopentane displayed *m*/*e* 84, 69, and 56 amu, the ratio of intensities of *m*/*e* 84 to 69 were diagnostic for the two compounds: 0.65 for 1-hexene and 0.25 for methylcyclopentane.

Crystallographic Studies. Crystal, data collection, and refinement parameters are given in Table 1. Suitable crystals were selected and mounted with epoxy cement to glass fibers. The unit-cell parameters were obtained by least-squares refinement of the angular settings of 24 reflections ($20° \le 2\theta \le 25°$). The systematic absences in the diffraction data are uniquely consistent with the space group *Pbca* for *RRSS*-[Ni(tmc)CH_3](BAr'_4), $CH_3Co(dmgBF_2)_2py$, and $CH_3Co(dmgBF_2)_2H_2O$ and $I4_1/a$ for $CH_3Co(dmgBF_2)_2PEt_3$. The structures were solved using direct methods, completed by subsequent difference Fourier syntheses, and refined by full-matrix least-squares procedures. Semiempirical absorption corrections were applied to *RRSS*-[Ni(tmc)CH_3](BAr'_4) but were not required for $CH_3Co(dmgBF_2)_2PEt_3$, $CH_3Co(dmgBF_2)_2py$, and $CH_3Co(dmgBF_2)_2PEt_3$ because there was less than 10% variation in the ψ-scan intensities. In the anion of *RRSS*-[Ni(tmc)CH_3](BAr'_4) the phenyl groups were fixed as rigid groups and the fluorine atoms of the perfluoromethyl groups were constrained to an idealized tetrahedron to conserve data. The carbon atom, C(9), in *RRSS*-[Ni(tmc)CH_3](BAr'_4) is disordered over two positions with an occupancy distribution of 60/40. The asymmetric unit of $CH_3Co(dmgBF_2)_2PEt_3$ consisted of two independent, but chemically equivalent molecules. There are two nitromethane solvent molecules in the asymmetric unit of $CH_3Co(dmgBF_2)_2py$. The pyridine ring in $CH_3Co(dmgBF_2)_2py$ was fixed as a rigid group to conserve data and refined isotropically along with the two solvent molecules. All other nonhydrogen atoms were refined with anisotropic displacement coefficients. The hydrogen atoms in *RRSS*-[Ni(tmc)CH_3](BAr'_4) were omitted and all other hydrogen atoms were treated as idealized contributions. All software and sources of the scattering factors are contained in the SHELXTL (5.1) program libraries (G. Sheldrick, Siemens XRD, Madison, WI).

Results and Discussion

Choice of Model Complexes. As cluster A in CODH appears to consist of a complex assembly of minimum stoichiometry Ni−X−Fe_4S_4, we deliberately began these studies with a monomeric nickel complex void of sulfur ligands. This approach allows us to systematically evaluate the role of the nickel primary coordination sphere and the covalent attachment

(15) Bakac, A.; Espenson, J. H. *J. Am. Chem. Soc.* **1986**, *108*, 713−718.

(16) Eisenberg, D. C.; Lawrie, C. J. C.; Moody, A. E.; Norton, J. R. *J. Am. Chem.* Soc. **1991**, *113*, 4888−4895.

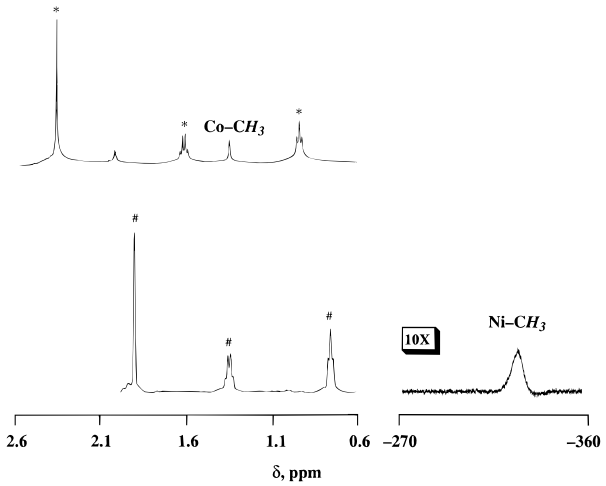

Figure 1. ^{1}H NMR spectra of $CH_3Co(dmgBF_2)_2PEt_3$ (10 mM) in acetone-d_6 before (A) and after (B) addition of 2 equiv of [Ni(tmc)]OTf: (*) $CH_3Co(dmgBF_2)_2PEt_3$, (#) $Co(dmgBF_2)_2PEt_3^-$.

of a Fe_4S_4 cluster to nickel,[17] respectively, in determining the course of the reactions. [Ni(tmc)](OTf)$_2$ was chosen because it is the only nickel complex in which the Ni(I) derivative has been crystallographically characterized and the corresponding methylnickel complex is stable;[6b] both the starting material and desired product of methyl transfer are isolable species. In choosing a suitable organocobalt complex, we required a system that allowed for variation of R and L substituents on cobalt and did not contain acidic hydrogens. The former criterion is paramount in the systematic evaluation of the effect of the steric and electronic parameters of the alkyl group and *trans* axial ligand in driving the kinetics of the reaction. The latter arises from the rapid reaction of [Ni(tmc)]OTf with protons, resulting in oxidation to Ni(II) with liberation of H_2.[8] (For example, $[CH_3Co([14]aneN_4)(H_2O)](OTf)_2$ and $CH_3Co(dmgH)_2py$ oxidize [Ni(tmc)]OTf in preference to methyl transfer.) Therefore, we replaced the protons of the pseudomacrocycle in $CH_3Co(dmgH)_2py$ with (formally) BF_2^+ to yield the macrocyclic complex, $CH_3Co(dmgBF_2)_2py$, first described by Schrauzer.[18]

Addition of $CH_3Co(dmgBF_2)_2L$ (L = PEt_3, py) to [Ni(tmc)]OTf resulted in an immediate color change from light green to blue-green. The electronic spectrum of the products was dominated by $Co(dmgBF_2)_2L^-$, with a λ_{max} at 640 nm ($\epsilon = 9 \times 10^3\ M^{-1}cm^{-1}$), produced in greater than 80% yield. Spectral titration of [Ni(tmc)]OTf with $CH_3Co(dmgBF_2)_2py$ or $CH_3Co(dmgBF_2)_2PEt_3$ displayed a limiting absorbance at 640 nm with [[Ni(tmc)]OTf]/[$CH_3Co(dmgBF_2)_2L$] equal to 2, establishing the stoichiometry of the reaction. NMR spectroscopy was necessary to determine the other reaction products, Figure 1. [Ni(tmc)]CH_3]OTf displayed a characteristic signal at δ −332 for the Ni−C*H*$_3$.[13]

This assignment was corroborated by two experiments. First, [Ni(tmc)CH_3]OTf was prepared independently from [Ni(tmc)](OTf)$_2$ and $(CH_3)_2Mg$ according to Barefield.[19] The *RRSS* and *RSRS* isomers displayed identical ^{1}H NMR chemical shifts for the Ni−C*H*$_3$ protons. The isomeric identity was established by the number of resonances for the tmc protons (Experimental Section). The *RSRS* isomer contains a mirror plane of symmetry and consequently exhibits seven resonances for the tmc protons. The *RRSS* isomer, lacking a mirror plane, displays 13 tmc resonances Alternatively, [Ni(tmc)CD_3]OTf was prepared from $CD_3Co(dmgBF_2)_2py$ and [Ni(tmc)]OTf. The ^{2}H NMR spectrum contained a single sharp resonance at δ −332 ($\Delta\nu_{1/2}$ = 140 Hz). Such a high-field resonance for the methyl protons is consistent with the spin state $S = 1$, which provides a significant Fermi contact contribution to the chemical shift. (To date, all five-coordinate derivatives of [Ni(tmc)(X)]OTf are high spin, even with strong field apical ligands.[8]) The ^{1}H NMR spectrum of the products also contained resonances attributed to [Ni(tmc)](OTf)$_2$. Because many of the species in solution were paramagnetic, it was not possible to quantify the Ni-containing products by NMR. The fact that one product was [Ni(tmc)CH_3]OTf was further corroborated by its characteristic reactions with electrophiles, H_2O and $HgCl_2$. Addition of H_2O to a $(CH_3)_2SO$ solution of [Ni(tmc)CD_3]OTf yielded [Ni(tmc)OH]OTf and CD_3H quantitatively.[19] Alternatively, addition of $HgCl_2$ to a $(CH_3)_2SO$ solution of [Ni(tmc)CH_3]OTf resulted in an immediate color change to red with precipitation of an off-white solid. The ^{1}H NMR spectrum of the solution contained a resonance for CH_3HgCl (d 0.76, $^2J_{^{199}Hg-H}$ = 222 Hz), in 50% yield based on $CH_3Co(dmgBF_2)_2py$.

The products and stoichiometry of the reaction are consistent with a three-step mechanism triggered by single electron transfer (SET) from [Ni(tmc)]OTf to $CH_3Co(dmgBF_2)_2L$, eqs 1−3. This

$$CH_3Co(dmgBF_2)_2L + Ni(tmc)^+ \xrightarrow{e^- \text{ transfer}} CH_3Co(dmgBF_2)_2L^- + Ni(tmc)^{2+} \quad (1)$$

$$CH_3Co(dmgBF_2)_2L^- \rightarrow Co(dmgBF_2)_2L^- + CH_3^\bullet \quad (2)$$

$$Ni(tmc)^+ + CH_3^\bullet \rightarrow Ni(tmc)CH_3^+ \quad (3)$$

mechanism is analogous to that proposed by Espenson and Bakac for the reaction of CH_3I with [Ni(tmc)]ClO_4. In this regard, the analogy of methylcobalamin serving as Nature's "CH_3I equivalent" appears valid. The reduced $CH_3Co(dmgBF_2)_2L^-$ is susceptible to facile CH_3−Co homolysis which generates free radicals and Co(I), $Co(dmgBF_2)_2L^-$.[20] In the final step, the radical is captured by a second equivalent of [Ni(tmc)]OTf to yield [Ni(tmc)CH_3]OTf. This colligation rate has been measured by Espenson and Bakac in aqueous media for 1-hexenyl$^\bullet$. At 25 °C, the rate of capture of 1-hexenyl$^\bullet$ by [Ni(tmc)]ClO_4 is $6 \times 10^7\ M^{-1}\ s^{-1}$.[15] To corroborate the production of free radicals in the present system, we employed (5-hexenyl)Co$(dmgBF_2)_2L$ derivatives in the reaction with [Ni(tmc)]OTf.

1-Hexenyl Radical Probe. The 5-hexenyl radical undergoes cyclization to the cyclopentylmethyl radical in H_2O with a rate constant of $2.2 \times 10^5\ s^{-1}$ at 25 °C.[21] Consequently, the corresponding 1-halo-5-hexenes have been used as probes. In instances where both the cyclized and uncyclized products are observed, the rate constant for radical capture has been determined.[22] (5-hexenyl)Co$(dmgBF_2)_2L$ was prepared by addition of 1-bromo-5-hexene to *in situ* generated solutions of $Co(dmgBF_2)_2L^-$. Alkylation of Co(I) derivatives proceeds through a S_N2 pathway resulting in no detectable rearrangement

(17) In this context, we are aware of one model complex that contains a Ni ion covalently linked to an Fe_4S_4 cluster. This report contains a crystal structure but no spectroscopic nor catalytic data. Osterloh, F.; Saak, W.; Haase, D.; Pohl, S. *J. Chem. Soc., Chem. Commun.* **1996**, 777−778.

(18) Schrauzer, G. N.; Windgassen, R. J. *J. Am. Chem. Soc.* **1966**, *88*, 3738−3743.

(19) D'Aniello, M. J.; Barefield, E. K. *J. Am. Chem. Soc.* **1976**, *98*, 1610−1611.

(20) (a) Lexa, D.; Savéant, J. *J. Am. Chem. Soc.* **1978**, *100*, 3220−3222. (b) Martin, B. D.; Finke, R. G. *J. Am. Chem. Soc.* **1990**, *112*, 2419−2420. (c) Elliot, C. M.; Hershenhart, E.; Finke, R. G.; Smith, B. L. *J. Am. Chem. Soc.* **1981**, *103*, 5558−5566.

(21) Chatgilialoglu, C.; Ingold, K. U.; Scaiano, J. C. *J. Am. Chem. Soc.* **1981**, *103*, 7739−7742.

(22) Samuels, G. J.; Espenson, J. H. *Inorg. Chem.* **1979**, *18*, 2587.

Table 2. Second-Order Rate Constants for the Reaction $RCo(dmgBF_2)_2L + 2[Ni(tmc)](OTf)$ at 25 °C[a]

R	L	solvent	$10^{-3}k_2$ (M^{-1} s^{-1})[b]
CH_3	py	$(CH_3)_2SO$	2.43(4)
CH_3CH_2	py	$(CH_3)_2SO$	7.88(4)
$(CH_3)_2CH$	py	$(CH_3)_2SO$	19.2(10)
CH_3	PEt_3	$(CH_3)_2CO$	5.01(18)
CH_3	py	THF	4.51(16)[c]
CH_3CH_2	py	THF	11.1(23)
$(CH_3)_2CH$	py	THF	56(5)
CH_3	PEt_3	THF	17.0(3)

[a] Minor secondary spectral changes, slower by at least a factor of 10, were observed in some cases. [b] Errors refer to standard deviations based on an average of six runs per [[Ni(tmc)]OTf]. [c] A nontrivial intercept value of 74 s^{-1} was observed when the k_{obs} values were plotted against [[Ni(tmc)]OTf].

of the olefin.[14] Reaction of (5-hexenyl)$Co(dmgBF_2)_2L$ with 2 equiv of [Ni(tmc)]OTf was carried out in $(CH_3)_2SO$ for L = py and acetone for L = PEt_3. In each case, the products were hydrolyzed and the volatile organics were analyzed by GC−MS. For L = py, methylcyclopentane was the only product detected. However, for L = PEt_3, methylcyclopentane and several hexadiene isomers were present in the GC−MS. Production of methylcyclopentane provides compelling evidence for a free radical intermediate. Despite attempts over a range of concentrations, we were unable to find conditions which produced both uncyclized and cyclized products. Consequently, the rate constant for 5-hexenyl radical capture by [Ni(tmc)]OTf in organic solvents could not be determined.

Kinetics. Stopped-flow measurements were conducted with an excess of [Ni(tmc)]OTf. Under these conditions pseudo-first-order kinetics were observed for at least 3 half-lives by monitoring the growth of $Co(dmgBF_2)_2L^-$ at the wavelength of largest absorbance change, near λ_{max} = 628 nm for L = PEt_3 and λ_{max} = 640 nm for L = py. The k_{obs} values obtained from these single-wavelength measurements agreed with those obtained from a global fit of the data from 450 to 750 nm. Over this 300-nm range isosbestic behavior was observed. Each k_{obs} value was determined by taking the mean of typically six values from individual runs. The reaction obeyed a second-order rate law (eq 4); second-order rate constants are listed in Table 2. The trend of rate constants, R = CH_3 < CH_3CH_2 < $(CH_3)_2CH$, L = py, is consistent with the relative stabilities of the corresponding alkyl radicals and is therefore in agreement with our proposed mechanism.[23] Bakac and Espenson have observed a similar trend for RX reduction by $[Ni(tmc)]ClO_4$.[15] The rate constants they measured in H_2O are less than an order of magnitude lower than our values in $(CH_3)_2SO$. This remarkable agreement lends further support for similar mechanisms for both systems.

Nucleophilic displacement of R−Co by [Ni(tmc)]OTf would be expected to result in a trend opposite that in Table 2. For example, Castro and Stolzenberg independently determined that $Ni(OEiBC)^-$, a Ni(I) tetrapyrrole, reacted with haloalkanes in the order CH_3 > primary > secondary > tertiary.[25] Furthermore, the small solvent dependence a factor of ca. 2 for THF vs DMSO of the rate constants in Table 2 argues against an S_N2 mechanism. Reactions of CH_3I with metal complexes of unit charge exhibit pronounced solvent effects, i.e. for CH_3I + $CpFe(CO)_2SPh^-$, $k_{DMSO}/k_{acetone}$ is 12.[24] Finally, for the methyl derivatives, k_2 for L = PEt_3 is *ca.* four times greater than k_2 for L = py. As discussed below, this difference in rate constants reflects the difference in one-electron reduction potentials of the cobalt complexes, with the L = PEt_3 complex more easily reduced.

Table 3. Electrochemical Data for $CH_3Co(dmgBF_2)_2L$ (L = PEt_3, py)

L	E_f, V[a]	
PEt_3	−1.02	quasi-irrev
py	−1.10	quasi-irrev

[a] Versus NHE in THF with internal Fc/Fc^+ as indicated in the Experimental Section.

$$\frac{d[Co(dmgBF_2)_2L^-]}{dt} = k_2[Ni(tmc)OTf][RCo(dmgBF_2)_2L] \quad (4)$$

Cyclic Voltammetry of $CH_3Co(dmgBF_2)_2L$ Complexes. We previously reported the CV for the L = py derivative in $(CH_3)_2SO$ at a sweep rate of 20 mV/s.[7] Under these conditions, a chemically irreversible reduction at −990 mV (vs Ag/AgCl) was attributed to an EC mechanism in which $CH_3Co(dmgBF_2)_2$-py is reduced to $CH_3Co(dmgBF_2)_2py^-$. The CH_3−Co bond of the latter species rapidly homolyzes to yield $Co(dmgBF_2)_2py^-$ and $CH_3^\bullet$. In accord with this mechanism, an anodic sweep revealed an oxidative process at −430 mV which was present only following the reductive process. The oxidative process is assigned to the Co(II)/Co(I) couple by comparison with an independently prepared sample of $Co(dmgBF_2)_2py$. The other alkylcobalt complexes exhibited identical reduction potentials under these conditions. Our qualitative CV observations agree well with those reported for methylcobalamin[20a] and methylcobinamide.[20b] In those studies, Lexa and Savéant and Finke, respectively, reported rate constants for the CH_3−Co(II) bond homolysis (k_{hom}) of 4400 s^{-1}. To compare these rate constants to the present system, CV experiments were performed in THF at fast sweep rates using microelectrodes. Instrumental limitations prevented sweep rates greater than 150 V/s from being accessed. These conditions were sufficient to observe up to 50% of the anodic current, i.e. i_c/i_a = 2, for the back oxidation of $CH_3Co(dmgBF_2)_2L^-$. By measuring the i_c/i_a ratio as a function of sweep rate, values of k_{hom} were extracted as described previously.[8] The rates of k_{hom} = 500 (L = py) and 300 s^{-1} (L = PEt_3) are an order of magnitude less than those of methylcobalamin and methylcobinamide. Furthermore, by sweeping at these higher rates, the formal potentials for the reductive process may be determined, Table 3. The py complex is 80 mV more difficult to reduce than the PEt_3 complex, and correspondingly, the rate of reduction by [Ni(tmc)]OTf is a factor of 4 slower. While the relative potentials of the [Ni(tmc)]OTf and $CH_3Co(dmgBF_2)_2L$ indicate the initial electron transfer step is endergonic by at least 290 and 370 mV (values are approximations because the CH_3Co(III/II) formal potentials are not known) for L = PEt_3 and py, respectively, the CH_3−Co(II) homolysis and CH_3−Ni formation are exergonic[26] and more than compensate for the unfavorable energetics of the first step.

Cyclic Voltammetry of [Ni(tmc)CH_3]OTf. [Ni(tmc)CH_3]-OTf displayed a chemically irreversible oxidation at 50 mV (sweep rate, 50 mV/s) yielding a species which upon subsequent cathodic scanning was reduced at −1.0 V, Figure 2. The latter

(23) Shi, S.; Bakac, A.; Espenson, J. H. *Inorg. Chem.* **1991**, *30*, 3410−3414.

(24) Ashby, M. T.; Enemark, J. H.; Lichtenberger, D. L. *Inorg. Chem.* **1988**, *27*, 191−197.

(25) (a) Helvenston, M. C.; Castro, C. E. *J. Am. Chem. Soc.* **1992**, *114*, 8490−8496. (b) Lahiri, G. K.; Schussel, L. J.; Stolzenberg, A. M. *Inorg. Chem.* **1992**, *31*, 4991−5000.

(26) The Ni−Bzl BDE in [Ni(tmc)Bzl]OTf has been determined to be 18 kcal/mol by kinetic measurements. J. Halpern and M. Schofield, private communication.

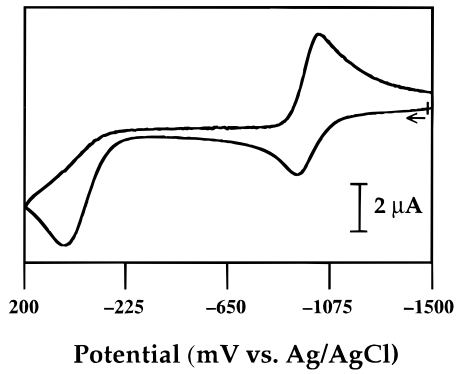

Figure 2. Cyclic voltammogram of [Ni(tmc)CH_3](OTf) in DMSO. Parameters are indicated in the Experimental Section. Peak assignments are contained in the text.

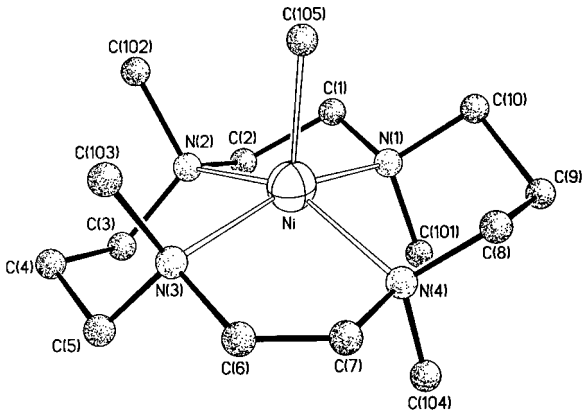

Figure 3. PLUTO drawing of the cation of [Ni(tmc)CH_3](BAr′$_4$). The minor isomer and hydrogen atoms are omitted for clarity.

event was assigned to the Ni(II)/Ni(I) couple.[8] The anodic peak was attributed to an EC mechanism entailing oxidation to [Ni(tmc)CH_3]$^{2+}$ followed by CH_3−Ni(III) homolysis yielding [Ni(tmc)]$^{2+}$ and $CH_3^{\bullet}$. Efforts to observe the back reduction in competition with homolysis by sweeping at scan rates up to 150 V/s were unsuccessful. Consequently, the lower limit for CH_3Ni(III) homolysis is at least $k_{hom} = 800\ s^{-1}$. This value is an order of magnitude greater than for the homolysis of another CH_3Ni(III), [CH_3Ni([14]aneN_4)](ClO_4)$_2$.[27] The difference in rates may reflect the greater steric crowding at nickel and consequently weaker CH_3Ni bond, in the *N*-methylated complex.

Molecular Structure of [Ni(tmc)CH_3](BAr′$_4$). Attempts to determine the molecular structure of [Ni(tmc)CH_3](X), X = OTf^-, PF_6^-, failed due to crystal twinning which resulted in data sets which could not be satisfactorily refined. Therefore, a large counteranion was sought which would significantly alter the crystal packing of the molecule. Crystals of [Ni(tmc)CH_3](BAr′$_4$) grown from THF−hexanes proved suitable for X-ray analysis. The crystal structure consists of discrete ions with no close contacts between Ni(tmc)CH_3^+ and BAr′$_4^-$. A view of the cation is presented in Figure 3 and selected metric parameters are contained in Table 4. Despite starting with isomerically pure *RSRS*-[Ni(tmc)](BAr′$_4$)$_2$, the Ni(tmc)CH_3^+ ion shows a 60:40 distribution of the *RSRS* and *RRSS* isomers of the tmc ligand. This is manifest in the central methylene carbon of one of the six-membered rings, C(9), which is disordered over two positions with the above occupancies. The geometry about the Ni ion is square pyramidal, with the four amine nitrogens providing basal ligation with Ni−N distances averaging 2.15(2) Å and the CH_3 in the apical position, Ni−C 2.04(1) Å. The Ni is displaced from the N_4 plane toward the alkyl ligand by 0.43 Å. The Ni−N distances are similar to those of other five-coordinate Ni(tmc)X^+ derivatives[28] such as the arylthiolates recently prepared by us, *RSRS*-[Ni(tmc)SC_6H_5]PF_6, Ni−N_{av}, 2.15(1) Å,[8] and in accord with the high-spin state. The Ni−C bond length is at the upper limits of the range for other Ni(II)−C(sp^3) lengths, 1.81−2.02 Å.[29] Recently, Latos-Grazynski has reported the only other structure of a paramagnetic organonickel(II) complex, (21-CH_3CTPP)Ni.[30] The N_3C coor-

Table 4. Selected Bond Distances (Å) and Bond Angles (deg) for [Ni(tmc)CH_3](BAr′$_4$), CH_3Co(dmgBF_2)$_2$(PEt_3), CH_3Co(dmgBF_2)$_2$py•2CH_3NO_2, and CH_3Co(dmgBF_2)$_2$(H_2O)

		[Ni(tmc)CH_3](BAr′$_4$)	
Ni−C(105)	2.04(1)	N(1)−Ni−N(2)	84.2(5)
Ni−N(1)	2.16(1)	N(2)−Ni−N(3)	91.7(5)
Ni−N(2)	2.14(1)	N(2)−Ni−N(4)	150.6(4)
Ni−N(3)	2.22(1)	N(3)−Ni−N(4)	84.9(4)
Ni−N(4)	2.10(1)	N(1)−Ni−N(4)	90.7(5)
		N(1)−Ni−C(105)	97.9(5)
		N(2)−Ni−C(105)	103.4(5)
		N(3)−Ni−C(105)	99.1(5)
		N(4)−Ni−C(105)	106.0(5)
		CH_3Co(dmgBF_2)$_2$(PEt_3)	
Co−C(15)	2.036(5)	N(1)−Co−N(2)	81.8(2)
Co′−C(15′)	2.038(4)	N(1′)−Co′−N(2′)	81.5(2)
Co−N(1)	1.857(4)	N(1)−Co−N(3)	98.3(2)
Co′−N(1′)	1.859(4)	N(1′)−Co′−N(3′)	98.2(2)
Co−N(2)	1.858(4)	N(2)−Co−N(4)	98.2(2)
Co′−N(2′)	1.862(4)	N(2′)−Co′−N(4′)	98.5(2)
Co−N(3)	1.862(4)	N(3)−Co−N(4)	81.2(2)
Co′−N(3′)	1.859(4)	N(3′)−Co′−N(4′)	81.5(2)
Co−N(4)	1.869(4)	C(15)−Co−P	179.6(2)
Co′−N(4′)	1.852(4)	C(15′)−Co′−P′	179.2(2)
Co−P	2.363(1)	N(1)−Co−P	90.5(1)
Co′−P′	2.371(2)	N(1′)−Co′−P′	92.6(1)
		N(2)−Co−P	96.0(1)
		N(2′)−Co′−P′	91.0(1)
		N(3)−Co−P	89.0(1)
		N(3′)−Co′−P′	92.6(1)
		N(4)−Co−P	94.4(1)
		N(4′)−Co′−P′	91.5(1)
		CH_3Co(dmgBF_2)$_2$py•2 CH_3NO_2	
Co−C(14)	2.007(8)	N(1)−Co−N(2)	81.3(3)
Co−N(1)	1.876(7)	N(1)−Co−N(3)	175.1(3)
Co−N(2)	1.851(7)	N(2)−Co−N(4)	176.2(3)
Co−N(3)	1.874(6)	N(3)−Co−N(4)	82.2(3)
Co−N(4)	1.846(7)	C(14)−Co−N(1)	89.4(3)
Co−N(5)	2.119(4)	C(14)−Co−N(2)	85.2(3)
		C(14)−Co−N(3)	85.8(3)
		C(14)−Co−N(4)	91.1(3)
		C(14)−Co−N(5)	179.7(3)
		CH_3Co(dmgBF_2)$_2H_2O$	
Co−C(9)	2.000(6)	N(1)−Co−N(2)	81.6(2)
Co−N(1)	1.866(4)	N(1)−Co−N(3)	179.9(2)
Co−N(2)	1.864(5)	N(2)−Co−N(4)	179.2(2)
Co−N(3)	1.854(5)	N(3)−Co−N(4)	82.0(2)
Co−N(4)	1.878(4)	C(9)−Co−N(1)	92.1(2)
Co−O(5)	2.127(4)	C(9)−Co−N(2)	87.7(2)
		C(9)−Co−N(3)	87.9(2)
		C(9)−Co−N(4)	93.0(2)
		C(9)−Co−O(5)	177.4(2)

(27) (a) Sauer, A.; Cohen, H.; Meyerstein, D. *Inorg. Chem.* **1988**, *27*, 4578. (b) Kelley, D. G.; Marchaj, A.; Bakac, A.; Espenson, J. H. *J. Am. Chem. Soc.* **1991**, *113*, 7583−7587.

(28) (a) Wagner, F.; Mocella, M. T.; D'Aniello, M. J.; Wang, A. H.-J.; Barefield, E. K. *J. Am. Chem. Soc.* **1974**, *96*, 2627−2635. (b) D'Aniello, M. J.; Mocella, M. T.; Wagner, F.; Barefield, E. K.; Paul, I. C. *J. Am. Chem. Soc.* **1975**, *97*, 192−194. (c) Lincoln, S. F.; Hambley, T. W.; Pisaniello, D. L.; Coates, J. H. *Aust. J. Chem.* **1984**, *37*, 713−723. (d) Crick, I. S.; Hoskins, B. F.; Tregloan, P. A. *Inorg. Chim. Acta* **1986**, *114*, L33−L34.

(29) Jolly, P. W. In *Comprehensive Organometallic Chemistry*; Wilkinson, G., Stone, F. G. A., Abel, E. W., Eds.; Pergamon: Oxford, 1982; Vol. 6, p 37.

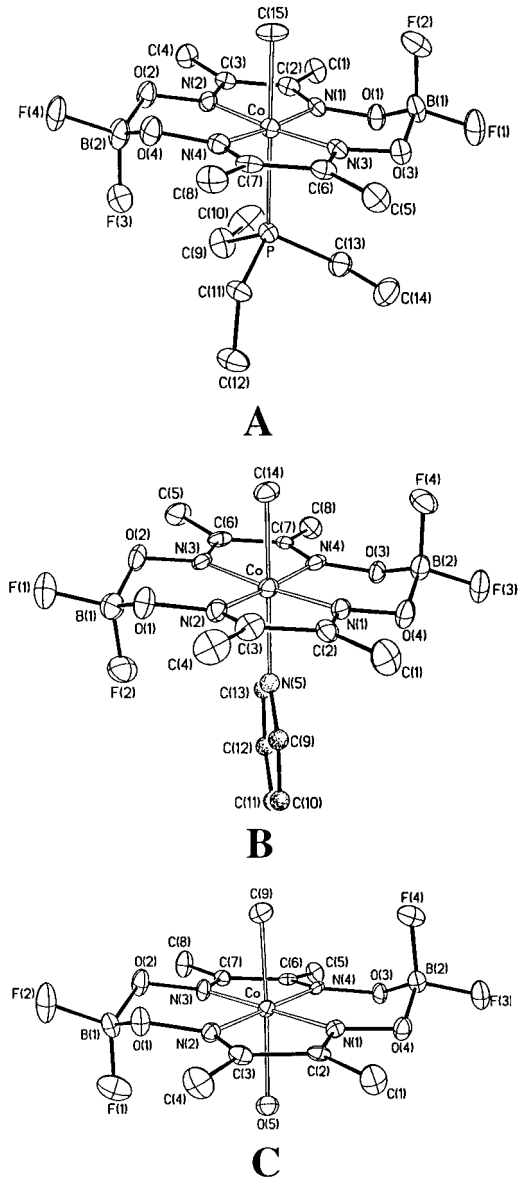

Figure 4. Thermal ellipsoid plots of (A) $CH_3Co(dmgBF_2)_2PEt_3$, (B) $CH_3Co(dmgBF_2)_2py\bullet 2CH_3NO_2$, and (C) $CH_3Co(dmgBF_2)_2H_2O$. Thermal ellipsoids are drawn at the 40% probability level. The solvent molecules in B and the hydrogen atoms are omitted for clarity.

dination core is essentially planar with the short Ni−C length of 2.005(6) Å reflecting constraints imposed by the macrocycle.

Molecular Structures of $CH_3Co(dmgBF_2)_2L$ (L = py, PEt_3, H_2O). The molecular structure of each derivative is displayed in Figure 4 with selected metric parameters contained in Table 4. This study is the first report of the structures of organocobalt complexes containing the bis(difluoroboryl)dimethylglyoximato macrocycle. The corresponding methylcobaloxime derivatives, L = py, PPh_3, PMe_3, and H_2O, have been crystallographically characterized previously.[31] In $CH_3Co(dmgBF_2)_2py\bullet 2CH_3NO_2$ and $CH_3Co(dmgBF_2)_2H_2O$ the macrocycles are in the extended chair conformations, i.e. one BF_2 resides below the plane defined by the four dimethylglyoximato nitrogens and one is above said plane. $CH_3Co(dmgBF_2)_2PEt_3$ crystallized with two independent molecules in the asymmetric unit cell. In general, the metric parameters for each are identical within experimental error; however, one molecule is in an extended chair conformation and the other in an extended boat (latter not shown). These distinct conformations appear to be a consequence of solid state effects. In solution at room temperature, facile equilibration between the two isomers occurs on the ^1H and ^{19}F NMR time scales. The plane of the pyridine ring in $CH_3Co(dmgBF_2)_2py$ is perpendicular to the plane defined by the cobalt and two boron atoms. The pyridine orientation is offset by 90° from that typically observed in $XCo(dmgH)_2py$ structures.[31a,32] The steric influence of the BF_2 groups is most likely responsible for this change. Rotation of the pyridine by 90° would result in short van der Waals' contacts between the fluorine and the pyridine *ortho* hydrogen. Table 5 lists comparative cobalt−ligand bond lengths for the bis(difluoroboryl)dimethylglyoximato and dimethylglyoximato complexes. The Co−C bond distances are approximately 2.00 Å and invariant to the other ligands on cobalt. The Co−N distances for the $(dmgBF_2)_2$ macrocycle are shorter by *ca.* 0.03 Å than for the corresponding $(dmgH)_2$ derivatives. This finding is consistent with the electronic spectra which display shifts to higher energy for the absorption bands of the $(dmgBF_2)_2$ complexes. While the Co−C bond length is insensitive to these changes at the cobalt,[33] the Co−L length responds significantly. The $(dmgBF_2)_2$ complexes have longer Co−L lengths, e.g., $CH_3Co(dmgH)_2(H_2O)$, Co−O, 2.058(3) Å; $CH_3Co(dmgBF_2)_2(H_2O)$, Co−O, 2.127(4) Å.

Table 5. Comparative Bond Lengths (Å) for $CH_3Co(dmgX)_2L$ Complexes

X	L	Co−C	Co−N_{av}	Co−L
BF_2	py	2.007(8)	1.861(13)	2.119(4)
H	py	1.998(5)	1.899(8)	2.068(3)
BF_2	H_2O	2.000(6)	1.865(9)	2.127(4)
H	H_2O	1.990(5)	1.890(9)	2.058(3)
BF_2	PEt_3	2.036(5)	1.861(8)	2.363(4)
		2.038(5)	1.858(8)	2.371(2)
H	PMe_3	2.011(3)	1.879(8)	2.291(1)
		2.019(3)	1.882(8)	2.295(1)
H	PPh_3	2.026(1)	1.890(10)	2.418(1)

Summary

The following are the principal findings and conclusions of this study.

(1) Methyl transfer from $CH_3Co(dmgBF_2)_2L$ to [Ni(tmc)]OTf occurs in high yield by a radical mechanism involving free methyl radicals. Support for the mechanism includes radical clock experiments using (5-hexenyl)$Co(dmgBF_2)_2L$ and kinetic measurements which are in accord with rate-limiting electron transfer. The trend of second-order rate constants for various alkyl groups parallels the relative stability of the corresponding free radicals. The rate constants are several orders of magnitude greater than the most efficient S_N2 methyl transfer reactions.[34] Curiously, the rates are similar to the value of 1.2 s^{-1} at 25 °C measured by Ragsdale for the reaction of methylated C/Fe-SP with reduced CODH.[5b]

(2) The electron transfer pathway is accessible in the present system due to favorable thermodynamics—the electron transfer

(30) Chmielewski, P. J.; Latos-Grazynski, L.; Glowiak, T. *J. Am. Chem. Soc.* **1996**, *118*, 5690−5701.

(31) (a) Bigotto, A.; Zangrando, E.; Randaccio, L. *J. Chem. Soc., Dalton Trans.* **1976**, 96−104. (b) Bresciani-Pahor, N.; Calligaris, M.; Randaccio, L.; Marzilli, L. G. *Inorg. Chim. Acta* **1979**, *32*, 181−187. (c) Bresciani-Pahor, N.; Randaccio, L.; Toscano, P. G.; Sandercock, A. C.; Marzilli, L. G. *J. Chem. Soc., Dalton Trans.* **1982**, 129−134. (d) McFadden, D. L.; McPhail, A. T. *J. Chem. Soc., Dalton Trans.* **1974**, 363−366.

(32) (a) Lenhert, G. P. *J. Chem. Soc., Chem. Commun.* **1967**, 980. (b) Adams, W. W.; Lenhert, G. P. *Acta Crystallogr.* **1973**, *B29*, 2412.

(33) (a) Rossi, M.; Glusker, J. P.; Randaccio, L.; Summers, M. F.; Toscano, P. J.; Marzilli, L. G. *J. Am. Chem. Soc.* **1985**, *107*, 1729−1738. (b) López, C.; Alvarez, S.; Font-Bardía, M. *J. Organomet. Chem.* **1991**, *414*, 245−259.

(34) Lewis, E. S.; Kukes, S.; Slater, C. D. *J. Am. Chem. Soc.* **1980**, *102*, 1619−1623.

step is only slightly endergonic as determined by the relative formal potentials of Ni(II/I) and CH_3Co(III/II). This reaction is energetically compensated by the CH_3-Ni bond forming step which is enthalpically favored[26] and therefore results in an overall process which is thermodynamically driven. The energetics of the enzyme are significantly different than those of the present model. Electron transfer is undoubtedly more endergonic (although the CH_3Co(III/II) potential for the C/Fe-SP has not been reported its value in other cobalamins is −1.36 V[20a]) due to the more modest cluster A reduction potential. However, again CH_3-Ni bond making may compensate for this enthalpic cost. Alternatively, Nature may have chosen methylcobalamin as the penultimate methyl donor for ACS precisely because its reduction potential is inaccessible by cluster A at kinetically relevant rates. The enzyme may be protecting itself from radical pathways and favoring two-electron events such as nucleophilic displacements. Clearly, a complete understanding of the mechanistic parameters of ACS awaits our ability to evaluate the role of the Fe_4S_4 cluster in catalysis.[17] Studies in progress are designed to evaluate the role of thiolate ligands to nickel and covalent attachment of a Fe_4S_4 cluster in modulating the methyl transfer reaction.

(3) The structure of a paramagnetic organonickel complex has been determined by X-ray diffraction. The Ni−C bond length of 2.04(1) Å is within the range of other Ni(II)−C(sp^3) bond lengths and shows little or no effect from the high-spin state of the metal.

Acknowledgment. This paper is dedicated to Professor James H. Espenson on the occasion of his 60th birthday for his many significant contributions to our understanding of alkyl transfer reactions. C.G.R. gratefully acknowledges the financial support of the National Science Foundation (OSR-9255223 and NYI Award, 1994−99), and the donors of The Petroleum Research Fund, administered by the American Chemical Society (27076-G3). A.M. and J.R.N. acknowledge the financial support of the National Institutes of Health (GM48537). We thank Dr. B. Plashko for assistance with the GC-MS experiments and Prof. M. M. Collinson for the use of the BAS 100 voltammetric analyzer.

Supporting Information Available: Tables containing the structure determination summary, atomic coordinates, bond lengths, and bond angles for [Ni(tmc)CH_3](BAr′$_4$), $CH_3Co(dmgBF_2)_2(PEt_3)$, $CH_3Co(dmgBF_2)_2(py)\bullet 2CH_3NO_2$, and $CH_3Co(dmgBF_2)_2(H_2O)$ (32 pages). See any current masthead page for ordering and Internet access instructions.

JA963061Z